

Radar-Based Multi-Target Localization and Vital Sign Monitoring

Yuping Shi¹, Qinwei Li¹, Hang Wu², Ming Yu^{2*}

¹Tianjin Key Laboratory for Advanced Signal Processing, School of Electronic Information and Automation, Civil Aviation University of China, Tianjin, China

²Systems Engineering Institute, Academy of Military Science, People's Liberation Army, Tianjin, China

Email: syp_6699@163.com, qw_li@cauc.edu.cn, 2008.wuhang@163.com, *yuming_1990@outlook.com

How to cite this paper: Shi, Y.P., Li, Q.W., Wu, H. and Yu, M. (2024) Radar-Based Multi-Target Localization and Vital Sign Monitoring. *Journal of Computer and Communications*, 12, 263-278.
<https://doi.org/10.4236/jcc.2024.1211018>

Received: November 15, 2024

Accepted: November 26, 2024

Published: November 29, 2024

Abstract

The frequency-modulated continuous wave (FMCW) radar, known for its high range resolution, has garnered significant attention in the field of non-contact vital sign monitoring. However, accurately locating multiple targets and separating their vital sign signals remains a challenging research topic. This paper proposes a scene-differentiated method for multi-target localization and vital sign monitoring. The approach identifies the relative positions of multiple targets using Range FFT and determines the directions of targets via the multiple signal classification (MUSIC) algorithm. Phase signals within the range bins corresponding to the targets are separated using bandpass filtering. If multiple targets reside in the same range bin, the variational mode decomposition (VMD) algorithm is employed to decompose their breathing or heartbeat signals. Experimental results demonstrate that the proposed method accurately localizes targets. When multiple targets occupy the same range bin, the mean absolute error (MAE) for respiratory signals is 3 bpm, and the MAE for heartbeat signals is 5 bpm.

Keywords

Frequency-Modulated Continuous Wave (FMCW) Radar, Multi-Target, Multiple Signal Classification (MUSIC), Variational Mode Decomposition (VMD)

1. Introduction

In recent years, with the increasing frequency of public health issues and growing awareness of personal health, health monitoring has garnered significant attention and importance. Heart rate and respiratory rate are indispensable components of

vital sign parameters and serve as common diagnostic indicators for numerous diseases. Healthcare professionals can assess the severity of a patient's condition based on these parameters [1]. In hospitals, real-time monitoring of vital signs is critical to ensuring patient recovery. Currently, clinical practices predominantly rely on contact-based monitoring devices such as electrocardiograms (ECG) and respiratory inductance plethysmography [2]. However, these methods often compromise patient comfort, restrict mobility, and pose risks of secondary injury, particularly for patients with surface wounds, such as burn victims. Furthermore, in emergency rescue scenarios such as fires or earthquakes [3], rapid localization of human targets is essential to facilitate timely rescue and maximize the chances of survival. Therefore, research into non-contact vital sign monitoring and target localization is highly necessary.

Current technologies for non-contact vital sign monitoring and target localization primarily include computer vision, thermal imaging modules, and radar systems [4] [5]. Each of these methods has its strengths and limitations. Computer vision achieves vital sign monitoring and target localization by analyzing changes in skin reflectivity and employing image processing techniques [6]. However, the use of cameras raises privacy concerns, limiting their practical applications. Thermal imaging modules [7] rely on the body's thermal radiation to distinguish targets from their surroundings but are susceptible to interference from ambient temperatures and other heat sources. In contrast, microwave radar [8] [9] detects phase changes caused by chest or heart movements, capturing signals through electromagnetic wave transmission and reception. It operates effectively in both daytime and nighttime conditions, enabling continuous, uninterrupted monitoring. Consequently, research on non-contact vital sign monitoring and target localization using microwave radar holds significant importance.

Currently, vital sign monitoring techniques for single individuals have become relatively mature, with common optimizations addressing specific challenges. For instance, improved variational mode decomposition (VMD) methods have been employed to mitigate the impact of respiratory harmonics on heartbeat signals [10], two-dimensional phase accumulation techniques enable efficient processing of multi-chirp data [11], and Kalman filters are used to track target positions while suppressing nonlinear noise caused by body movements by subtracting displacement signals [12]. However, when monitoring multiple patients in a hospital ward simultaneously, deploying multiple radar systems incurs high costs and results in low utilization rates of radar modules. Consequently, some research teams have shifted their focus to multi-target vital sign monitoring. The Fraunhofer Institute for High Frequency Physics and Radar Techniques developed a 120 GHz MIMO radar system that utilizes 3D image reconstruction to separate and detect the respiratory and heartbeat signals of two subjects located in different range bins [13]. Researchers from the China Coal Technology and Engineering Group achieved target localization using permutation entropy combined with K-means++ clustering [14]. Similarly, Zhang *et al.* employed Pearson correlation coefficients to

determine the actual number of targets and utilized back-projection (BP) to calculate their positions [15].

However, the afore mentioned studies primarily focus on scenarios where multiple targets are located at different range bins. In practical situations, hospital beds are typically at the same height, leading to targets being positioned at the same range. Therefore, this study explores target localization and vital sign monitoring for multiple targets located within the same range bin.

To address the above challenges, this paper proposes a radar-based method for vital sign monitoring using a differentiation framework. The method detects the target's range bin through Range FFT and determines the direction of targets using the Multiple Signal Classification (MUSIC) algorithm [16], thereby completing target localization. When multiple targets are located at different range bins, phase signals from multiple range bins can be obtained. Bandpass filters are then applied to the phase signals of each range bin to extract the corresponding breathing and heartbeat signals. If multiple targets reside within the same range bin, the breathing and heartbeat signals are first separated using bandpass filters. The VMD algorithm is subsequently employed to extract the breathing or heartbeat signals of each individual target. By correlating the signal amplitude with the energy intensity of the signal source, the method effectively matches the targets' locations with their respective vital sign signals.

The structure of this study is as follows: Section II provides a detailed explanation of the principles underlying target localization and vital sign monitoring. Section III describes the experimental validation of the proposed method and presents the corresponding results. Section IV concludes the paper with a summary of the findings.

2. Research Method

Frequency-modulated continuous wave (FMCW) radar enables vital sign monitoring by detecting phase variations in FMCW signals within specific range gates, caused by subtle movements of the human chest and heart.

2.1. Radar Localization Principle

FMCW radar periodically transmits frequency signals that increase linearly over time. When the target is stationary, the millimeter-wave radar's range resolution is on the order of centimeters, while the amplitude of chest or heart movements is on the millimeter scale. Therefore, the human body can be approximated as a static target, enabling static target localization.

The periodically transmitted linearly increasing frequency signals, known as chirp signals, can be expressed as:

$$S_{TX}(t) = A_{TX} \exp\left(j\left(2\pi f_c t + \pi\gamma t^2 + \varphi(t)\right)\right) \quad (1)$$

where f_c is the starting frequency, B is the transmission signal bandwidth, T_c is the pulse duration, $\gamma = B/T_c$ is the linear frequency modulation slope, and

φ is the initial phase. When the human target is stationary, the radial distance from the radar to the human body is R_c , $0 \leq t \leq T_c$. The echo signal received by the antenna after a time delay of $\tau = 2R_c / c$ (where c is the speed of light) is given by:

$$S_{RX}(t) = A_{RX} \exp\left(j\left(2\pi f_c(t-\tau) + \pi\gamma(t-\tau)^2 + \varphi(t-t_d)\right)\right) \quad (2)$$

The mixer combines the transmitted signal with the echo signal, and after passing through a low-pass filter, the intermediate frequency (IF) signal is obtained. The phase of the IF signal corresponds to the phase difference between the transmitted signal and the echo signal, which can be expressed as:

$$\begin{aligned} S_{IF}(t) &= A_T A_R \exp\left(j\left(2\pi\gamma\tau t + 2\pi f_c\tau + \pi\gamma t^2 + \Delta\varphi(t)\right)\right) \\ &\approx A_T A_R \exp\left(j\left(2\pi\gamma\tau t + 2\pi f_c\tau\right)\right) \\ &A_T A_R \exp\left(j2\pi(f_b t + \phi_b)\right) \end{aligned} \quad (3)$$

Since $\pi\gamma t^2$ is very small, it can be approximated $\Delta\varphi(t)$ as negligible. Based on the range-related effect, the term can also be ignored. Thus, the frequency and phase can be expressed as: $f_b = 2\gamma R_c / c$, $\phi_b = 4\pi f_c R_c / c$. By calculating the FFT of the intermediate frequency (IF) signal, its frequency spectrum can be expressed as:

$$S_{IF}(f) = A_T A_R T_c \exp(j\phi_b) \text{sinc}(T_c(f - f_b)) \quad (4)$$

By using incoherent accumulation, the distance corresponding to the maximum energy point can be determined. The frequency f_b of the intermediate frequency (IF) signal is obtained by finding the peak index of the frequency spectrum. Based on the formula: $R_c = cf_b / 2\gamma$.

The MUSIC algorithm performs eigenvalue decomposition on the covariance matrix of the data received by the array antenna. From the matrix of eigenvectors corresponding to different eigenvalues, it distinguishes between the signal subspace and the noise subspace. The eigenvectors corresponding to the larger eigenvalues form the signal subspace, while those corresponding to the smaller eigenvalues constitute the noise subspace. Due to the orthogonality between the signal and noise subspaces, the spatial spectrum (or beamforming spectrum) can be calculated. By searching for peaks in the spectrum, the direction of the target can be determined. Therefore, by applying the MUSIC algorithm to process the target phase signal from range bin, the direction information of the target can be obtained.

2.2. Signal Preprocessing

After determining the target range bin, the phase information for that range bin is obtained using the arctangent function:

$$\varphi_b = \tan^{-1} \frac{\text{imag}(\text{data})}{\text{real}(\text{data})} \quad (5)$$

Since the phase obtained by the arctangent function lies within the range of $[-\pi, \pi]$, any phase values exceeding this range will be wrapped back into it, causing phase ambiguity. To resolve this, phase unwrapping is applied to restore the phase to its original form, resulting in phase changes that contain the target's vital sign information, as shown in the (6), where $\Delta\phi(t)$ represents the difference between two adjacent phase values:

$$\Delta\phi(t) = \begin{cases} \phi(t) - \phi(t-1), & |\phi(t) - \phi(t-1)| \leq \pi \\ \phi(t) - \phi(t-1) + 2\pi, & \phi(t) - \phi(t-1) < -\pi \\ \phi(t) - \phi(t-1) - 2\pi, & \phi(t) - \phi(t-1) > \pi \end{cases} \quad (6)$$

Since heartbeats cause weaker fluctuations compared to chest movements, this paper implements phase differencing in the signal processing process by subtracting consecutive phase values from the unwrapped phase. This approach effectively eliminates baseline phase drift and suppresses low-frequency components, such as the respiratory signal. As a result, high-frequency components, such as the heartbeat signal, are enhanced, facilitating better identification of the heartbeat signal.

2.3. Vital Sign Monitoring

The chest displacement caused by human breathing ranges from 1 to 12 mm, while the heart displacement due to heartbeat is much smaller, ranging from 0.1 to 0.5 mm. The human respiratory rate is between 16 to 20 breaths per minute, while the heart rate typically ranges from 60 to 100 bpm. These two frequencies are significantly different from each other. A bandpass filter can extract signals within a specific frequency range. Therefore, a bandpass filter can be used to initially separate the respiratory and heartbeat signals from the radar data.

Due to varying scenarios, the processing methods also differ. When targets are at different range bins, the phase signals of different range bins can be processed, and the bandpass filter can separate the respiratory and heartbeat signals for each target. However, when multiple targets are located at the same range bin, after using the bandpass filter to separate the respiratory and heartbeat signals, the VMD algorithm is employed to decompose the breathing or heartbeat signals of each individual target.

The VMD algorithm iteratively searches for the optimal solution of the model to determine the center frequency and bandwidth of each component. After the modalities are demodulated into baseband signals, they become smooth signals. Moreover, the VMD algorithm can determine the number of modes to be decomposed, exhibiting strong adaptive characteristics. It overcomes the modal aliasing issue present in the Empirical Mode Decomposition (EMD) algorithm, making VMD more suitable for the practical needs of this study.

After obtaining the vital sign signals of each target, the heart rate and respiratory rate of each target can be estimated by calculating the frequency peak with the maximum amplitude in the spectrum, as shown in the following formula:

$$V_{hr} = f_{hr} * 60 \tag{7}$$

where V_{hr} represents the heart rate value, and f_{hr} is the frequency peak in the spectrum corresponding to the heart rate.

In addition, when multiple targets are located at the same range bin, the issue of matching the targets with their corresponding vital sign signals arises. By sorting the spectral amplitudes obtained from the MUSIC algorithm along with the amplitudes of the vital sign signals, the correspondence between each target and its respective vital sign signal can be established. The flowchart of the proposed method is shown in **Figure 1**.

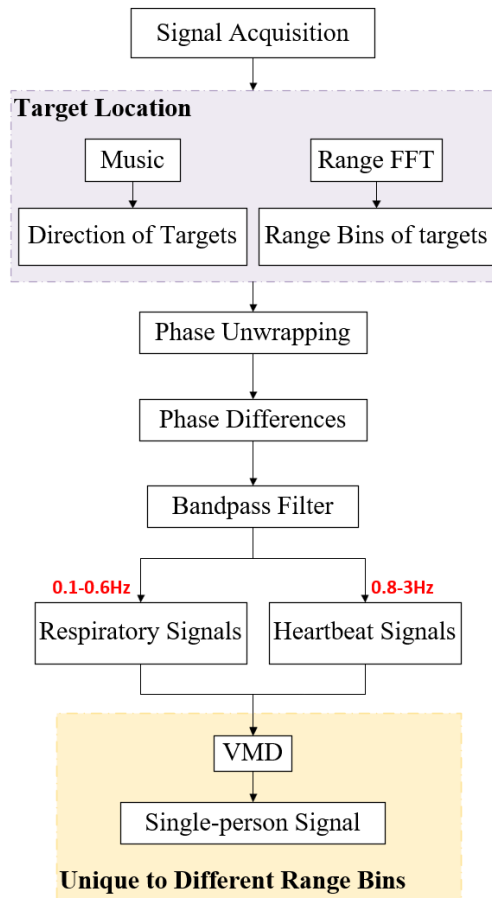


Figure 1. The flowchart of the proposed method.

3. Experimental Setup and Processing

3.1. Experimental Setup

In this study, radar echo data and gold standard data were collected using a radar module, a fingertip oximeter, and a respiratory monitoring belt. The radar module consists of a radar board and a data acquisition board. The radar board is the IWR6843ISK-ODS from Texas Instruments (TI), and the data acquisition board is the DCA1000EVM from TI. The radar board is tuned to a frequency range of 60 - 64 GHz and includes 4 receiving antennas and 3 transmitting antennas. Radar

echo data is collected via the Samtec interface and stored in binary files. The fingertip oximeter is the CMS50E module from CONTEC, with data stored in CSV format at a sampling frequency of 1 sample per second, meeting the experimental requirements. The respiratory monitoring belt is a product developed by Renhe Technology, with monitoring results transmitted via Bluetooth. The equipment diagram is shown in **Figure 2**. In the diagram, the radar board and data acquisition board are shown in **Figure 2(a)**, the fingertip oximeter is shown in **Figure 2(b)**, and the respiratory monitoring belt is shown in **Figure 2(c)**.

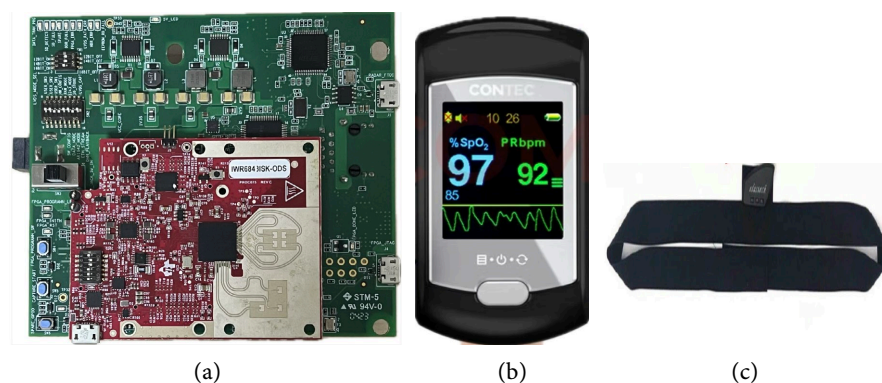


Figure 2. The equipment diagram. (a) The radar board and data acquisition board. (b) The fingertip oximeter. (c) The respiratory monitoring belt.

3.2. Signal Acquisition

The data acquisition scenario in this study involves three targets sitting in front of the radar board, each wearing a fingertip oximeter and a respiratory monitoring belt to record ground truth values. The relative positions of multiple targets are shown in **Figure 3**. In **Figure 3(a)**, all three targets are located at the same range bin, with the distance between the radar board and the human body set to 0.8 meters. In **Figure 3(b)**, the three targets are located at different range bins, with the radar board distances to the individuals being 0.6 meters, 1.4 meters, and 1.9 meters, respectively. During data collection, the radar board sampling rate was set



Figure 3. Experimental scenario. (a) Targets located at the same range bin. (b) Targets located at different range bins.

to 4 MHz, with 200 sampling points, 2 chirps, and 1024 frames, resulting in a total collection duration of 1 minute.

3.3. Experimental Processing

The radar echo data is stored in two channels, real and imaginary, resulting in a data length of 6,553,600 points. The radar echo signal is shown in **Figure 4**. Before processing the data, the real and imaginary channel data are combined into a complex form. Since this study aims to detect vital sign signals from multiple targets, static clutter removal is applied prior to signal processing to enhance the vital sign signals.

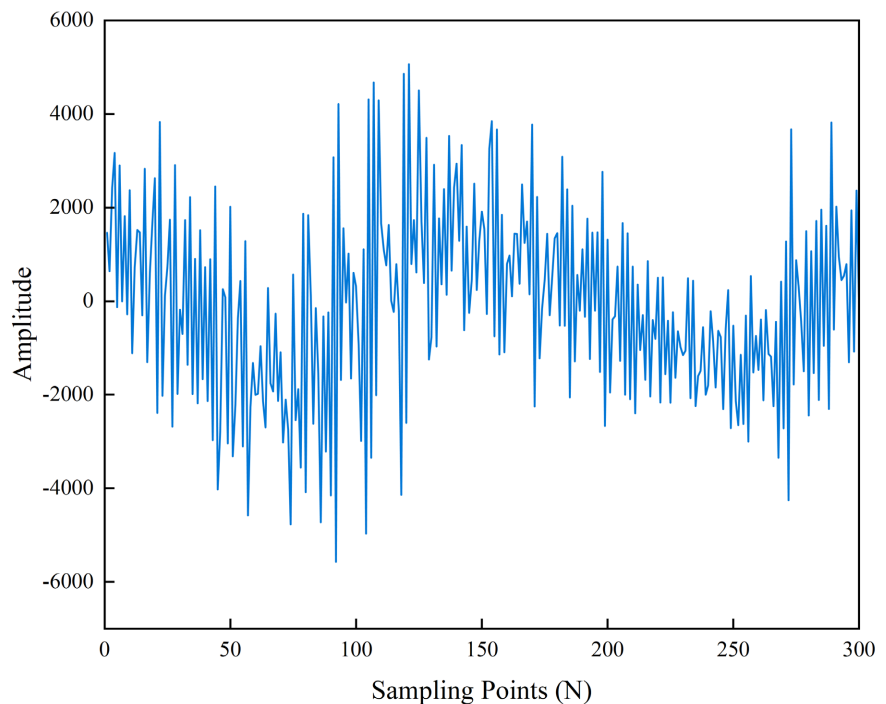
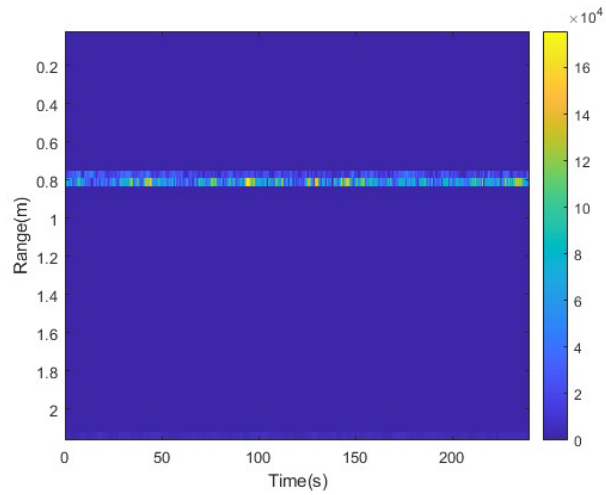


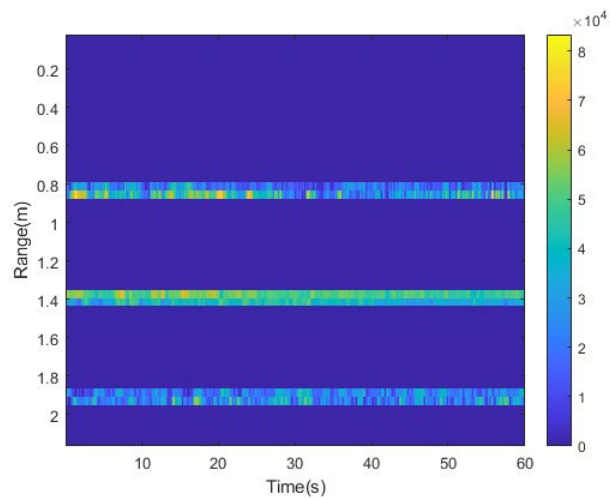
Figure 4. Radar echo signal.

The echo signals are arranged into a matrix form with fast time and slow time dimensions. The fast time dimension, representing data from different range bins, is subjected to a Range FFT, completing the conversion from the time domain to the frequency domain. This process yields a Range FFT image, as shown in **Figure 5**. **Figure 5(a)** shows the image when all three targets are located at the same range bin, while **Figure 5(b)** shows the image when the targets are located at different range bins. In both cases, the Range FFT images clearly display the data.

When multiple targets are located at the same range bin, it is necessary to distinguish them based on the direction of targets. Validation was conducted using data where multiple targets are located at different range bins. The MUSIC algorithm was employed to determine the direction of targets, and the results are shown in **Figure 6**. Specifically, **Figure 6(a)** illustrates the scenario where multiple targets are in the same range bin, while **Figure 6(b)** depicts the scenario where

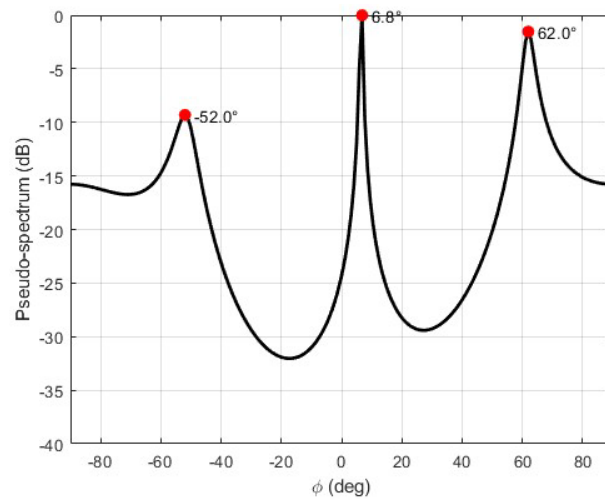


(a)



(b)

Figure 5. Range FFT image. (a) Targets located at the same range bin. (b) Targets located at different range bins.



(a)

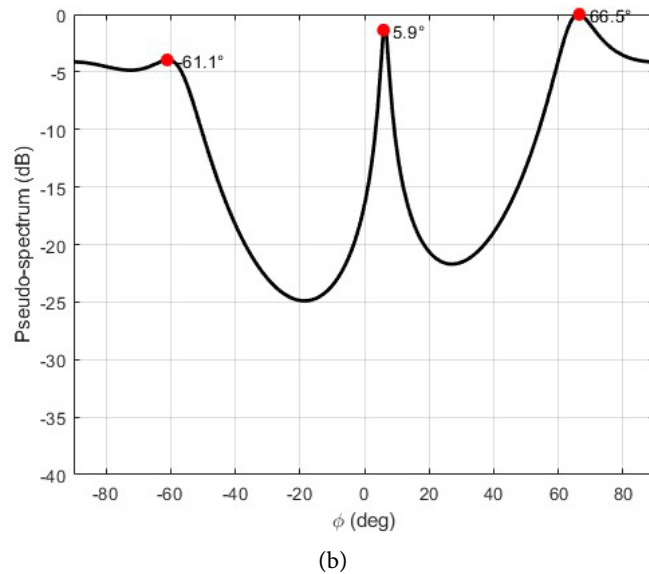


Figure 6. Direction of targets. (a) Targets located at the same range bin. (b) Targets located at different range bins.

targets are in different range bins. For targets in different range bins, the target closer to the radar board exhibits a larger signal amplitude, with the strongest energy corresponding to an echo signal from 66.5° . Additionally, the amplitudes of three signals decrease progressively, further verifying the effectiveness of the MUSIC algorithm. In this study, the number of signal sources for the MUSIC algorithm was set to 3, with 4 array elements and 1024 sampling points. This approach successfully enables the localization of multiple targets within the same range bin.

After determining the target's range information, the phase signal corresponding to the identified range cell is extracted. Due to the presence of phase wrapping, phase unwrapping is required to restore the signal to its original form. Phase differencing is then applied to enhance the target's heartbeat signal and eliminate phase drift, completing the data preprocessing.

The band-pass filter for the respiratory signal is set to a frequency range of 0.1 - 0.6 Hz, while for the heartbeat signal, the filter is set to a frequency range of 0.8 - 3 Hz. These band-pass filters effectively separate the respiration and heartbeat signals. The signal waveforms before and after filtering are shown in **Figure 7**. Specifically, **Figure 7(a)** displays the signal prior to bandpass filtering, while **Figure 7(b)** illustrates the respiration signal after bandpass filtering, demonstrating the effect of the filtering process.

When multiple targets are located at the same range bin, the VMD algorithm is used to separate the vital sign signals of these targets. During the implementation of the VMD algorithm, a secondary penalty factor needs to be determined. To avoid mode mixing and excessive computational load, the alpha parameter is set to 50,000, which corresponds to the length of the input signal. To reduce noise interference, the fidelity coefficient τ is set to 0, and the convergence condition ϵ is set to 10^{-7} . After obtaining the vital sign signals, the breathing rate and heart

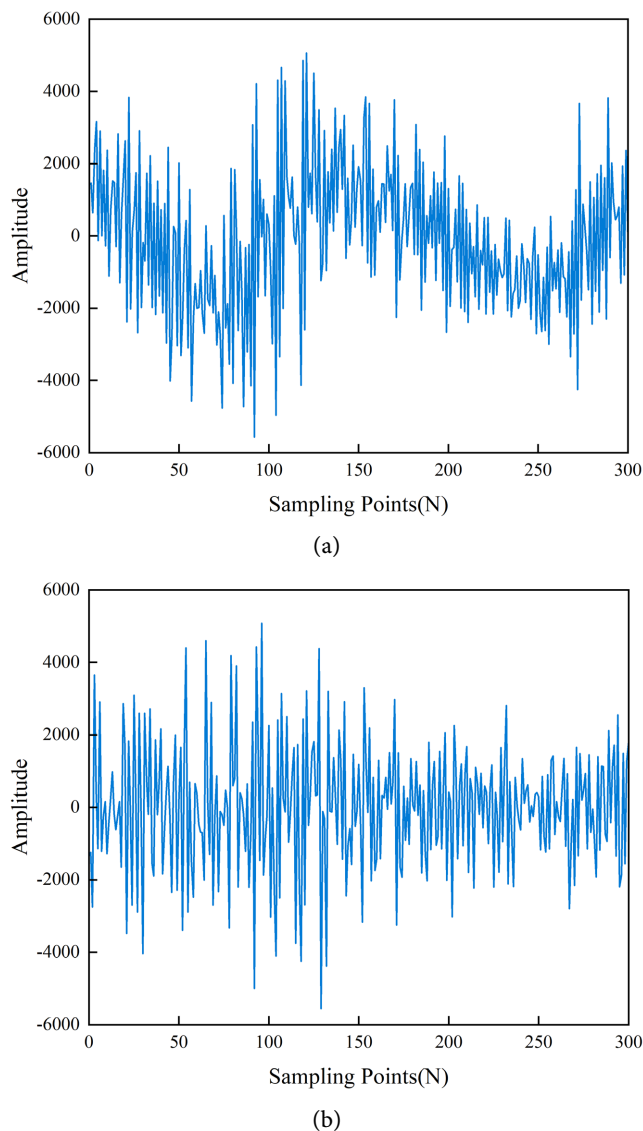


Figure 7. Signal waveforms before and after filtering. (a) The signal prior to bandpass filtering. (b) The respiration signal.

rate of each target are determined by identifying the peak frequency in the signal's spectrum. As shown in **Figure 8**, when the peak frequency is 1.07 Hz, the corresponding heart rate is 64.2 bpm.

3.4. Results

The detection results for the three individuals at different range bins are 0.69 meters, 1.37 meters, and 1.93 meters, achieving a tracking accuracy of 94%. The vital sign signals are shown in **Figure 9**. The mean absolute error (MAE) represents the average absolute difference between the true physiological measurements of the targets and the monitoring results obtained using the proposed method. For the case where the three individuals are at the same range bin, the MAE for the breathing rate is 3 bpm, and the MAE for the heart rate is 5 bpm.

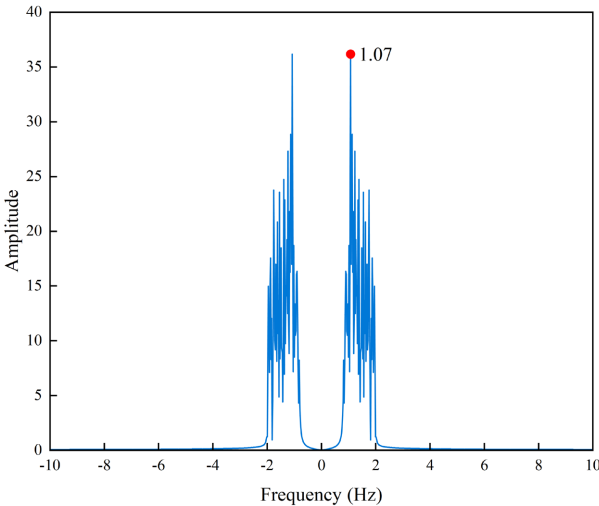
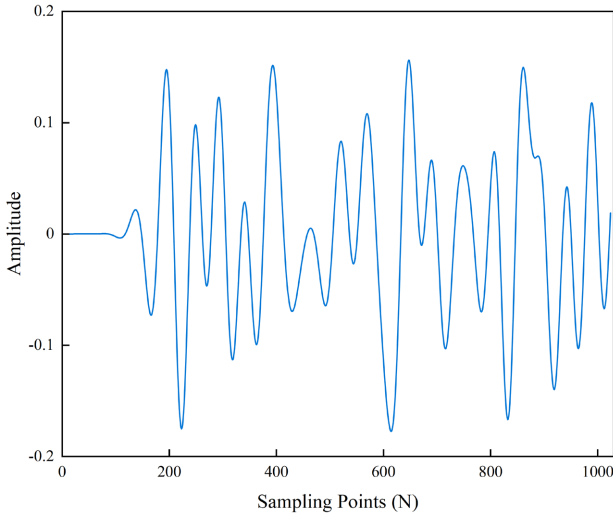
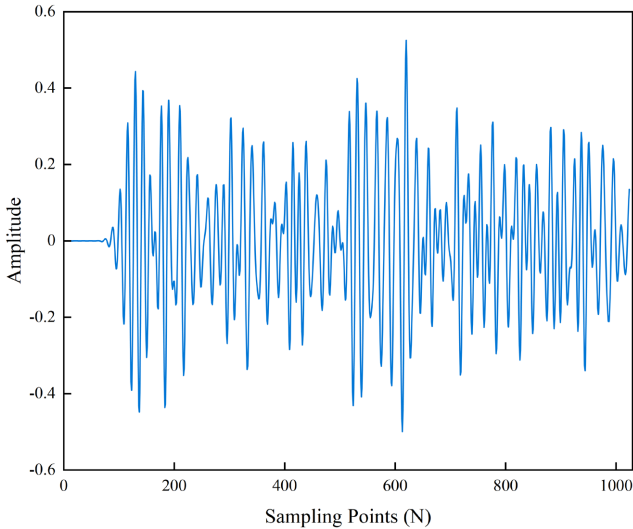


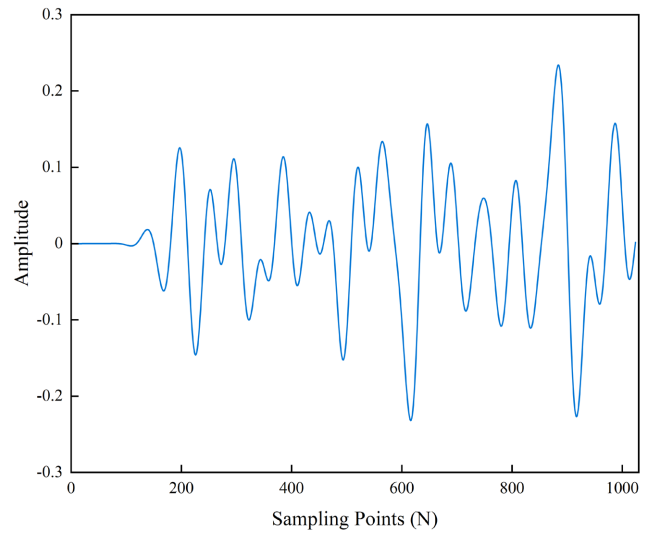
Figure 8. The Signal's Spectrum.



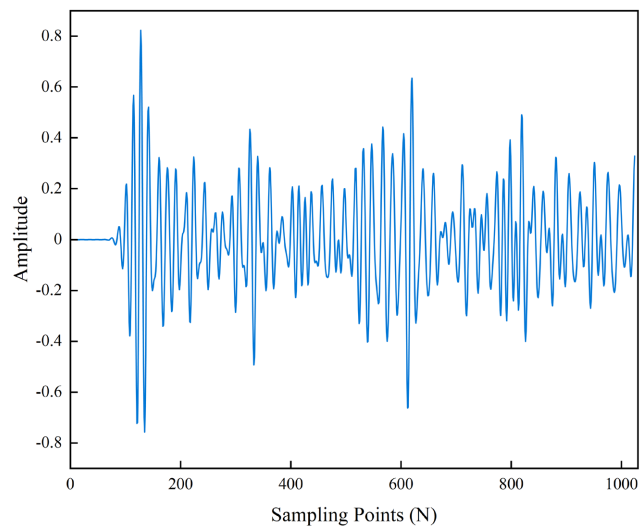
(a)



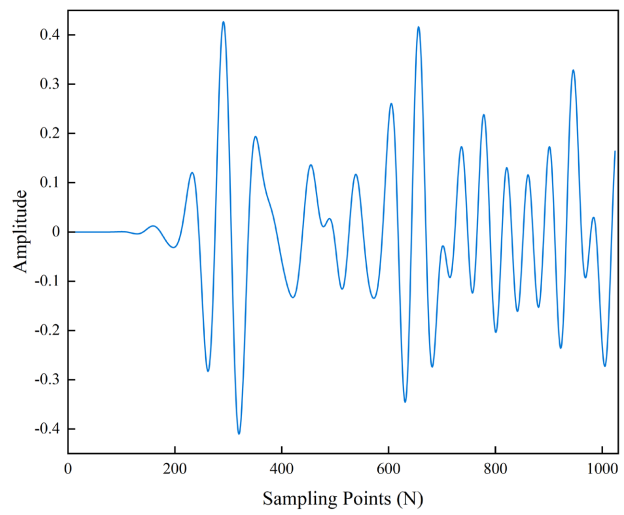
(b)



(c)



(d)



(e)

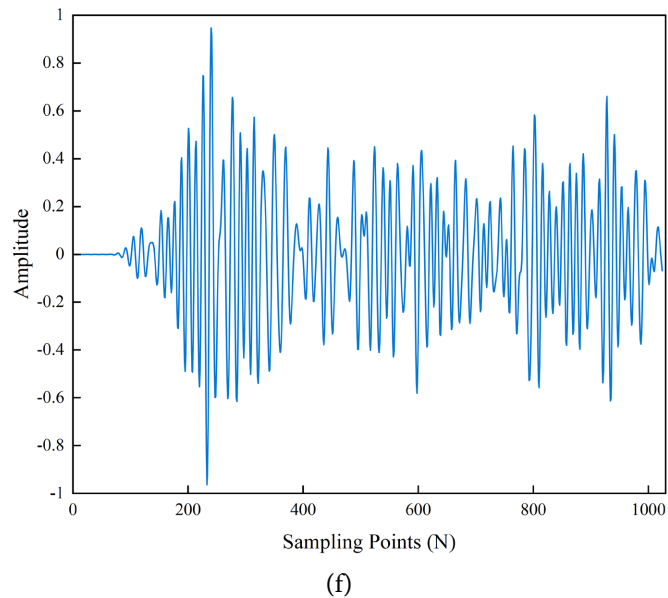


Figure 9. Vital sign signals. (a) The first target’s respiratory signal. (b) The first target’s heartbeat signal. (c) The second target’s respiratory signal. (d) The second target’s heartbeat signal. (e) The third target’s respiratory signal. (f) The third target’s heartbeat signal.

When the individuals are at different range bins, the MAE for the breathing rate is 2 bpm, and the MAE for the heart rate is 4 bpm. These results demonstrate that the proposed method effectively addresses the separation of vital sign signals and the positioning of multiple targets within the same range bin.

4. Conclusion

The method for multi-target positioning and vital sign monitoring based on FMCW radar proposed in this paper reduces costs and improves radar utilization. Through signal processing techniques, the processing results can be quickly obtained, with the entire process taking only 8.6 seconds, enabling real-time monitoring of patients’ physiological parameters. The use of scenario-specific processing methods eliminates the limitation of relative positions for multiple targets. Additionally, radar-based vital sign monitoring often faces the issue of mismatched patient identities and physiological information; however, the amplitude matching method proposed in this paper effectively addresses this problem. The signal processing method proposed in this paper achieves high accuracy for target positioning and vital sign monitoring. In the future, by extracting distance-angle signals from human targets, more accurate monitoring can be realized in multi-target, same-distance scenarios.

Acknowledgements

Thanks for Tianjin Education Commission. This paper is supported by “Tianjin Education Commission Research Program Project” funded by the Tianjin Education Commission (No. 2023KJ226).

Conflicts of Interest

The authors declare no conflicts of interest regarding the publication of this paper.

References

- [1] Nicolò, A., Massaroni, C., Schena, E. and Sacchetti, M. (2020) The Importance of Respiratory Rate Monitoring: From Healthcare to Sport and Exercise. *Sensors*, **20**, Article 6396. <https://doi.org/10.3390/s20216396>
- [2] Singh, A., Rehman, S.U., Yongchareon, S. and Chong, P.H.J. (2021) Multi-Resident Non-Contact Vital Sign Monitoring Using Radar: A Review. *IEEE Sensors Journal*, **21**, 4061-4084. <https://doi.org/10.1109/jsen.2020.3036039>
- [3] Pramudita, A.A., Lin, D., Hsieh, S., Ali, E., Ryanu, H.H., Adiprabowo, T., et al. (2022) Radar System for Detecting Respiration Vital Sign of Live Victim behind the Wall. *IEEE Sensors Journal*, **22**, 14670-14685. <https://doi.org/10.1109/jsen.2022.3188165>
- [4] Wang, F., Wu, C.M., Horng, T., Tseng, C., Yu, S., Chang, C., et al. (2020) Review of Self-Injection-Locked Radar Systems for Noncontact Detection of Vital Signs. *IEEE Journal of Electromagnetics, RF and Microwaves in Medicine and Biology*, **4**, 294-307. <https://doi.org/10.1109/jerm.2020.2994821>
- [5] Yan, J., Zhang, G., Hong, H., Chu, H., Li, C. and Zhu, X. (2019) Phase-Based Human Target 2-D Identification with a Mobile FMCW Radar Platform. *IEEE Transactions on Microwave Theory and Techniques*, **67**, 5348-5359. <https://doi.org/10.1109/tmtt.2019.2939523>
- [6] Li, Y., Wei, M., Chen, Q., Zhu, X., Li, H., Wang, H., et al. (2023) Hybrid D1DCnet Using Forehead iPPG for Continuous and Noncontact Blood Pressure Measurement. *IEEE Sensors Journal*, **23**, 2727-2736. <https://doi.org/10.1109/jsen.2022.3230210>
- [7] Negishi, T., Abe, S., Matsui, T., Liu, H., Kurosawa, M., Kirimoto, T., et al. (2020) Contactless Vital Signs Measurement System Using RGB-Thermal Image Sensors and Its Clinical Screening Test on Patients with Seasonal Influenza. *Sensors*, **20**, Article 2171. <https://doi.org/10.3390/s20082171>
- [8] Schroth, C.A., Eckrich, C., Kakouche, I., Fabian, S., von Stryk, O., Zoubir, A.M., et al. (2024) Emergency Response Person Localization and Vital Sign Estimation Using a Semi-Autonomous Robot Mounted SFCW Radar. *IEEE Transactions on Biomedical Engineering*, **71**, 1756-1769. <https://doi.org/10.1109/tbme.2024.3350789>
- [9] Wang, K., Zeng, Z. and Sun, J. (2019) Through-Wall Detection of the Moving Paths and Vital Signs of Human Beings. *IEEE Geoscience and Remote Sensing Letters*, **16**, 717-721. <https://doi.org/10.1109/lgrs.2018.2881311>
- [10] Qiao, L., Wang, Z., Xiao, B., Shu, Y., Luan, X., Shi, Y., et al. (2023) Spectral Unmixing Successive Variational Mode Decomposition for Robust Vital Signs Detection Using UWB Radar. *IEEE Transactions on Instrumentation and Measurement*, **72**, 1-13. <https://doi.org/10.1109/tim.2023.3274171>
- [11] Sun, L., Huang, S., Li, Y., Gu, C., Pan, H., Hong, H., et al. (2020) Remote Measurement of Human Vital Signs Based on Joint-Range Adaptive EEMD. *IEEE Access*, **8**, 68514-68524. <https://doi.org/10.1109/access.2020.2985286>
- [12] Xu, D., Yu, W., Wang, Y. and Chen, M. (2024) Vital Signs Detection in the Presence of Nonperiodic Body Movements. *IEEE Transactions on Instrumentation and Measurement*, **73**, 1-16. <https://doi.org/10.1109/tim.2024.3450071>
- [13] Wang, S., Kueppers, S., Cetinkaya, H. and Herschel, R. (2019) 3D Localization and Vital Sign Detection of Human Subjects with a 120 GHz MIMO Radar. 2019 20th International Radar Symposium (IRS), Ulm, 26-28 June 2019, 1-6.

<https://doi.org/10.23919/irs.2019.8768192>

- [14] Zhang, Y., Ma, Y., Yu, X., Wang, P., Lv, H., Liang, F., *et al.* (2021) A Coarse-To-Fine Detection and Localization Method for Multiple Human Subjects under Through-Wall Condition Using a New Telescopic SIMO UWB Radar. *Sensors and Actuators A: Physical*, **332**, Article ID: 113064. <https://doi.org/10.1016/j.sna.2021.113064>
- [15] Zhang, J., Qi, Q., Cheng, H., Sun, L., Liu, S., Wang, Y., *et al.* (2023) A Multi-Target Localization and Vital Sign Detection Method Using Ultra-Wide Band Radar. *Sensors*, **23**, Article 5779. <https://doi.org/10.3390/s23135779>
- [16] Lee, H., Kim, B., Park, J. and Yook, J. (2019) A Novel Vital-Sign Sensing Algorithm for Multiple Subjects Based on 24-GHz FMCW Doppler Radar. *Remote Sensing*, **11**, Article 1237. <https://doi.org/10.3390/rs11101237>